



EFFECTS OF A QUENCHED DISORDER ON WAVE PROPAGATION IN EXCITABLE MEDIA

I. SENDIÑA-NADAL, V. PÉREZ-MUÑUZURI, M. GÓMEZ-GESTEIRA,
A. P. MUÑUZURI and V. PÉREZ-VILLAR

*Grupo de Física non Lineal, Facultade de Física,
Universidade de Santiago de Compostela, 15706 Santiago de Compostela, Spain*

D. VIVES*, F. SAGUÉS*, J. CASADEMUNT† and J. M. SANCHO†

**Departament de Química Física,*

†Departament d'Estructura i Constituents de la Matèria,

Universitat de Barcelona, Av. Diagonal 647, 08028 Barcelona, Spain

L. RAMÍREZ-PISCINA

*Departament de Física Aplicada, Universitat Politècnica de Catalunya,
Av. Dr. Gregorio Marañón 44, 08028 Barcelona, Spain*

Received 15 November, 1998; Revised 19 January, 1999

The behavior of autowaves under the effect of a quenched disorder is studied in the framework of the light-sensitive Belousov–Zhabotinsky reaction. This allows us to introduce spatial disorder on the excitability by projecting patterns of light transmittance. In particular, we have selected a dichotomic random distribution of levels of transmittance. If the two values of transmittance are equally probable and allows wave propagation without breaking the waves, we find an opposite effect on the wave front velocity and shape depending on the considered dimension. On the other hand, if one of the two values of the transmittance distribution is set on the nonexcitable region, percolation phenomena can arise by changing the number of excitable sites. The different addressed situations are analytically interpreted giving theoretical predictions for the experimental and numerical results.

1. Introduction

Wave propagation in homogeneous excitable media has been the focus of study in the last years [Tyson & Keener, 1988; Meron, 1992]. Propagation of excitable waves through nonhomogeneous media has also been extremely treated; the interaction of waves and inert obstacles giving rise to anchoring [Allesie *et al.*, 1973; Spach *et al.*, 1981; Muñozuri *et al.*, 1998] or breaking of planar fronts [Karma, 1993; Agladze *et al.*, 1994; Gómez-Gesteira *et al.*, 1994; Starobin & Starmer, 1996]. Nowadays, the current interest has changed to the understanding of spatio-temporal structures in modulated

media [Sendiña-Nadal *et al.*, 1997; Armero *et al.*, 1996, 1997] and fluctuating media [Maselko & Showalter, 1991; Jung, 1993; Jung & Mayer-Kress, 1995; Sendiña-Nadal *et al.*, 1998a, 1998b; Kádár *et al.*, 1998; Wang *et al.*, 1999].

The influence of fluctuations on nonlinear systems has been the subject of intense experimental and theoretical investigations from different points of view, i.e. stochastic resonance [Wiesenfeld & Moss, 1995; Gammaitoni *et al.*, 1998] and noise-induced transitions [Horsthemke & Lefever, 1984]. On the other hand, front roughness induced by fluctuations has received increasing attention [Family & Vicsek, 1991; Zhang *et al.*, 1992; Barabasi &

Stanley, 1995]. In particular, the quenched versions of both Edwards–Wilkinson (EW) [1982] and Kardar–Parisi–Zhang equations [1986] have been analyzed when applied to kinetic roughening induced by time-independent disorder [Natterman *et al.*, 1992; Amaral *et al.*, 1994].

Here, we consider time-independent random spatial fluctuations of the excitability in the BZ reaction. Their effects on wave propagation are discussed. In Sec. 2 are introduced the experimental and numerical setup. Section 3 is devoted to a particular case of random fluctuations, namely, a dichotomic distribution of the excitability. 1D and 2D propagation cases are treated separately as they are affected by spatial fluctuations in a different way. In Sec. 4, a particular case of Sec. 3 is considered where one of the values of our two-state model prevents wave propagation giving rise to percolation phenomena.

2. Experimental and Numerical Setup

Experiments were performed by using the photo-sensitive version of the Belousov–Zhabotinsky (BZ)

reaction. In this reaction–diffusion system, the catalyst ruthenium bipyridil ($\text{Ru}(\text{bby})_3$) presents two states of oxidation that, in the redox process, promote either the production of the activator (HBrO_2) or the inhibitor (Br^-) species. In the illuminated BZ reaction, the Ru^{+2} is excited,

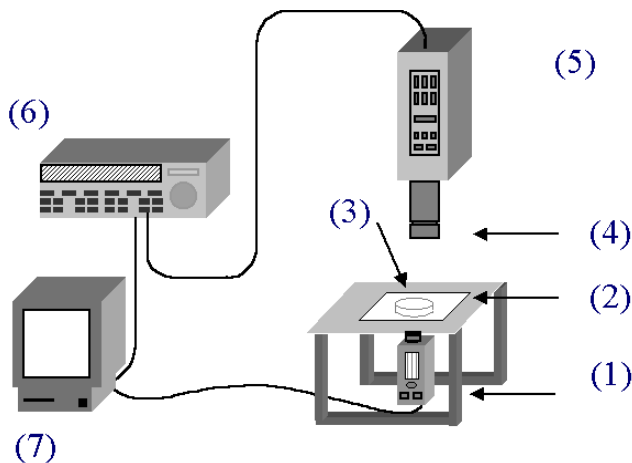


Fig. 1. Experimental setup. (1) Video Projector. (2) Milky glass. (3) Reaction. (4) Filter at 450 nm. (5) CCD camera. (6) Video. (7) PC.

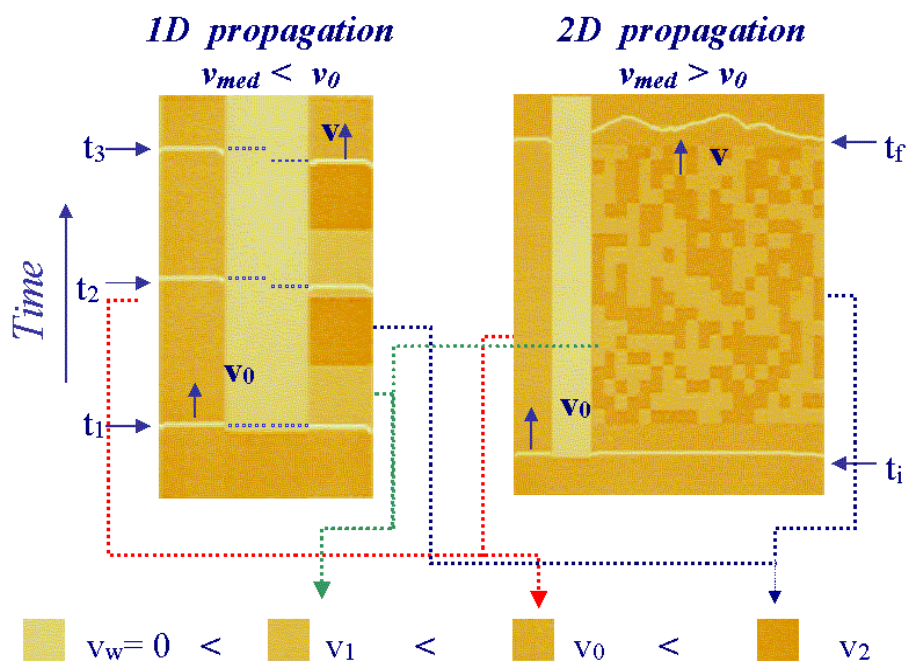


Fig. 2. Wave front propagation on a light-sensitive medium with a dichotomic random distribution of levels of transmittance. The images present the characteristic yellow color of the catalyst. Left: 1D setup. An initial flat front (t_0) splits into two, and were represented at three different times. The front which propagates through the inhomogeneous part undergoes an appreciable delay with respect to the other one (t_3). Stripe width in the direction of propagation $l = 1.1$ cm. Right: 2D setup. An initial flat front (t_i) gets rough in the randomly illuminated zone and goes faster than in the homogeneous part (t_f); Square size $l = 2.3$ mm and size of the medium in the transversal direction to the propagation 5.4 mm. Bottom: a sample of the light transmittances used in the patterns with the corresponding wave velocities.

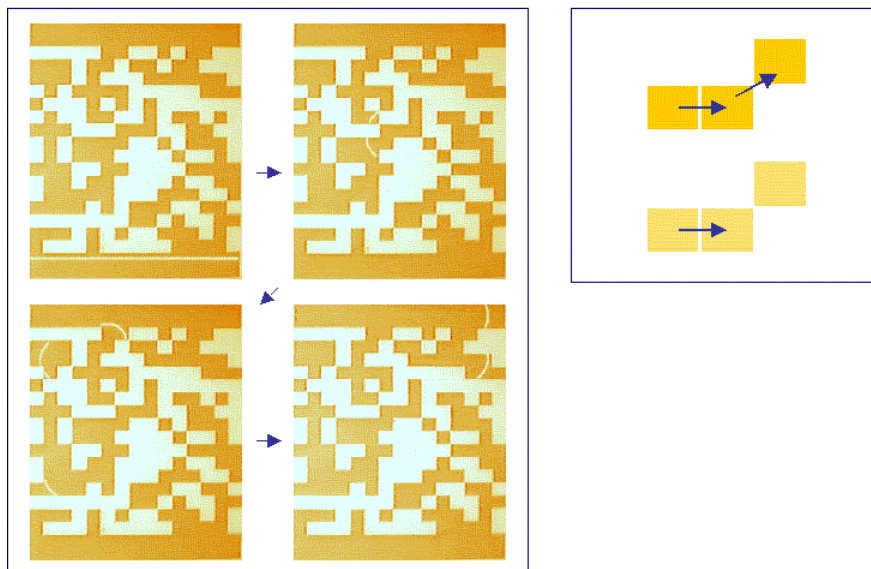


Fig. 3. Four different snapshots of the propagation of a wave front through a medium consisting of a random distribution of excitable squares (dark yellow) in a nonexcitable medium (light yellow). Propagation is only permitted through the excitable sites. An initial planar front (first panel) begins to propagate upwards. The wave breaks up into several parts which propagate through the lattice. The second panel corresponds to a moment where only two segments are present. Only one segment reaches the upper side first (third panel), whereas the others wander around the lattice until they disappear (last panel). Arrows indicate the time evolution corresponding to times: 0 s, 778 s, 1068 s, 1405 s. Proportion of excitable squares $p = 0.5$; size of squares, 3 mm; medium size, 4.5 cm \times 6 cm; light intensity through dark squares, 250 $\mu\text{W}/\text{cm}^2$, and through light ones, 750 $\mu\text{W}/\text{cm}^2$. Next to this time evolution is plotted schematically the two types of connectivity between cells. The first one takes place in the experiment shown in the figure on the left.

producing extra Br^- which decreases the excitability of the system and, consequently, the propagation velocity of the autowaves [Muñuzuri *et al.*, 1996; Ram-Reddy *et al.*, 1994]. In this way, it is possible to control the local excitability of the system by changing the intensity of the applied illumination. The Ru complex was immobilized in a silica-gel matrix (using a solution of 15% sodium silicate, 0.71 mM $\text{Ru}(\text{bpy})_3^{2+}$ and 0.18 M H_2SO_4 ; preparation as in [Yamaguchi *et al.*, 1991] in a Petri dish (diameter, 14 cm; thickness, 1 mm). The solution (initial concentrations: 0.18 M KBr, 0.33 M malonic acid, 0.39 M NaBrO_3 and 0.69 M H_2SO_4) was poured onto the gel. The temperature was kept constant at $25 \pm 1^\circ\text{C}$. The different parts of the setup are shown in Fig. 1. The reaction was exposed (from below) to spatially inhomogeneous light transmitted from a video projector, marked (1) in Fig. 1. The beam passed first a diffusion screen (2), then the Petri dish (3), the interference filter (4) (450.6 nm; transmission 56%), and, finally, a CCD (Charge Coupled Device) camera (5) for image recording (6) [Muñuzuri *et al.*, 1996b, 1997]. The images were digitized by an image-acquisition card and analyzed on a PC (7).

In order to introduce a spatial variation on the wave propagation conditions of the inhomogeneous medium, a transmission function $T(x, y)$ on an eight-bit gray-scale between 0 and 255 was generated in the PC and then transmitted through the video projector. The distribution function $T(x, y)$ directly fixes the light intensity reaching the medium (medium excitability decreases as light intensity increases [Sendiña *et al.*, 1997; Ram-Reddy *et al.*, 1994]).

Depending on the considered nonuniform situations, $T(x, y)$ exhibits different configurations and patterns. Figure 2 shows wave propagation through a medium with a random dichotomous distribution of the excitability. For this configuration, we considered two different scenarios. In both cases, the medium was split in two parts, the leftmost homogeneous and the rightmost nonhomogeneous, separated by a vertical, completely unexcitable, strip with higher illumination. In the quasi-one-dimensional configuration, horizontal stripes of random dichotomous illumination, with the same average light intensity as in the homogeneous part, introduced the disorder. The two-dimensional setup was prepared similarly, now randomly distributed

squares of two possible light intensities are projected. The transmission function is given by,

$$T(x, y) = \begin{cases} T_0 & \text{homogeneous medium} \\ 0 & \text{central strip} \\ T_0 + \delta T \cdot \eta(x, y) & \text{inhomogeneous medium} \end{cases}$$

where x is the transversal direction to front propagation, T_0 is the mean transmittance, and $\eta(x, y) = \pm 1$ is a two-valued random number of zero spatial average. Below Fig. 2 is shown the color scale of the light transmittances used with the corresponding velocities. When a medium with nonexcitable clusters is considered, $T(x, y)$ reproduces a two-dimensional dichotomous random distribution of dark and light squares (black and white from now on) of transmittances T_b and T_w , respectively, chosen in such a way that the wave cannot propagate through the white squares (the lighter ones in Fig. 3). Opposite to the other situation, the probability of one type of squares is permitted to vary from 0 to 1. Next to this figure two different types of connection between cells are shown for our two-dimensional square lattice. By changing the value of T_b we can select the actual connectivity of the lattice. For low values (low transmittance, upper connection), waves can propagate from a black site to both the nearest black site (through the common side) and to next-nearest black neighbors (through the vertex in common). For high values (high transmittance, lower connection), waves can only transit between black sites with a common side.

The typical experimental procedure consisted in generating a planar wave front at the bottom-side of the medium and observing its upward evolution along the vertical axis.

Numerical simulations were performed with a two-variable Oregonator model adapted to our photosensitive medium [Krug *et al.*, 1990] which in dimensionless form reads

$$\begin{aligned} \frac{\partial u}{\partial t} &= \frac{1}{\varepsilon} \left(u - u^2 - (fv + \phi(x, y)) \frac{u - q}{u + q} \right) + D_u \nabla^2 u \\ \frac{\partial v}{\partial t} &= (u - v) + D_v \nabla^2 v \end{aligned} \quad (1)$$

where u , respectively v , describe HBrO_2 , respectively catalyst, concentrations. D_u and D_v are the diffusion coefficients of both variables. f , q and ε are parameters related to the kinetics of the Belousov–Zhabotinsky reaction. $\phi(x, y)$ represents the light-induced flow of Br^- and it is directly proportional to $T(x, y)$. We employed an explicit

finite-difference scheme with mesh size 0.3 and time step 0.001 and no-flux boundary conditions. Due to finite-size effect limitations results were averaged over 10 runs for each value of the probability p of black squares.

3. Random Dichotomous Distribution of the Excitability

Typical experimental observations are shown in Fig. 2. For the two different scenarios, two non-interacting wave fronts propagate from an initially planar wave (at times t_0 and t_i). In the quasi-1D arrangement [Fig. 2(a)], the planar front emerging from the inhomogeneous part (at time t_2) is observed to move slower, in average, than the one which propagates under uniform illumination corresponding to the spatial average of the inhomogeneous region. Contrarily, in 2D [Fig. 2(b)], distorted, although still well-defined wave front, propagates faster (time t_f).

3.1. Theoretical approach

In order to establish our theoretical scenario it is needed to state clearly the conditions with which our experimental and numerical study must comply. This will allow us to interpret the observed results in terms of generic kinematic arguments widening in this way the scope of our study beyond the particular randomness realization analyzed here. Listing them separately:

- (i) We restrict ourselves to thin fronts measured on the length scale introduced by the disorder.
- (ii) The autowave speed adapts quasi-adiabatically to the local illuminating conditions, both experimentally and numerically,
- (iii) We assume that the disorder amplitude, i.e. a measure of the dispersion of local velocities in our two-state model, is small.

In a 1D situation, and invoking conditions (i) and (ii) above, the propagating interface can be viewed as a point-like object which follows instantaneously a spatial profile of velocity $v(y) = v_0 + \delta v(y)$, which is two-valued and characterized by:

$$\begin{aligned} \langle v(y) \rangle &= 0 \\ \langle v(y) \rangle^2 &= (\delta v)^2 \end{aligned} \quad (2)$$

If L is large enough compared to the spatial correlations of the disorder and under self-averaging

conditions, it is possible to relate \bar{v} to an ensemble average in each point, that is,

$$\frac{1}{\bar{v}} = \left\langle \frac{1}{v(y)} \right\rangle \quad (3)$$

Substitution of $v(y)$ and taking as a common factor v_0 results in:

$$\left\langle \frac{1}{v(y)} \right\rangle = \frac{1}{v_0} \left\langle \frac{1}{1 + \frac{\delta v}{v_0}} \right\rangle \quad (4)$$

Considering $\delta v(y)$ to be bounded by $|\delta v(y)| < v_0$, the Taylor series expansion of the right part of this equation is,

$$\left\langle \frac{1}{v(y)} \right\rangle = \frac{1}{v_0} \sum_{n=0}^{\infty} (-1)^n \left\langle \left(\frac{\delta v}{v_0} \right)^n \right\rangle \quad (5)$$

which can be computed exactly for the two-state model considered here with $\delta v \equiv \pm \Delta v$

$$\left\langle \frac{1}{v(y)} \right\rangle = \frac{1}{v_0} \sum_{n=0}^{\infty} \left(\frac{\Delta v}{v_0} \right)^{2n} \quad (6)$$

It immediately follows from this Taylor series,

$$\left\langle \frac{1}{v(y)} \right\rangle = \frac{1}{v_0} \left(\frac{1}{1 - \left(\frac{\Delta v}{v_0} \right)^2} \right). \quad (7)$$

So, we have just related the time-averaged velocity to the statistical moments of the disorder giving a reduced velocity,

$$\frac{\bar{v} - v_0}{v_0} = - \left(\frac{\Delta v}{v_0} \right)^2 \quad (8)$$

For the 2D case, under the above conditions of our theoretical scenario, the use of the linear speed-curvature relation is justified, also well-known as first-order eikonal equation [Zykov, 1980; Pertsov *et al.*, 1997; Wellner & Pertsov, 1997]. This equation gives the normal velocity of the autowave in terms of its local plane-wave value corrected by a curvature term. Besides, by invoking condition (ii), the local velocity is assumed to be at any time fixed by the space-dependent illumination, so translating such a relation into Cartesian coordinates for the position of the front, denoted $y = h(x, t)$, we have

$$h_t = v(x, h) \sqrt{1 + (h_x)^2} + D \frac{h_{xx}}{1 + (h_x)^2} \quad (9)$$

where D is an effective diffusion coefficient and, in general, a function of diffusion coefficients of the species involved in the front propagation. Developing the eikonal equation under a small-gradient approximation and noting that $v(x, h) = v_0 + \delta v(x, h)$ we have

$$h_t = v_0 + \frac{v_0}{2} (h_x)^2 + D h_{xx} + \delta v(x, h) \quad (10)$$

where only the leading nonlinear term h_x^2 was retained and an extra multiplicative term $(h_x)^2 \delta v(x, h)$ was neglected for weak enough disorder amplitudes. Notice that, written in this way and after some trivial reparametrization to get rid of the trivial v_0 term, this equation strongly resembles the well-known KPZ model for the propagation of random interfaces [Kádár *et al.*, 1986]. [Kerstein & Ashurst, 1992] dealt with interfaces propagating in randomly advected media. They focussed their scaling analysis on the limit of frozen flows, which is completely equivalent to our scenario of quenched disorder. Under these conditions their main result reads $S = 1 + \beta Q^{4/3}$ [Kerstein & Ashurst, 1992]. Where S is the relative wave velocity and Q represents a relative measure of the randomness in the medium. In our notation $S \equiv v/v_0$ and $Q \equiv |\Delta v|/v_0$ the above expression becomes

$$\frac{\bar{v} - v_0}{v_0} = \beta \left[\left(\frac{\Delta v}{v_0} \right)^2 \right]^{2/3} \quad (11)$$

3.2. Results

The theoretical predictions, represented respectively by Eqs. (8) and (11), are compared with the numerical and experimental results in Fig. 4. For the 1D case, [Fig. 4(a)], the theoretical prediction is the continuous line of slope -1 . Numerical results approach better to this prediction whereas experimental ones deviate more as the amplitude of disorder increases. This is due to unavoidable experimental limitations in light dispersion and intrinsic inaccuracies in velocity measurements. The effect of light dispersion is associated to the production of inhibitor which is continuously produced in the brighter squares and tends to invade the darker ones, thus, increasing the *effective* value of the transmittance there. This effect becomes more important as the amplitude of the disorder increases. Therefore, the corresponding mean value T_0 of the transmission function

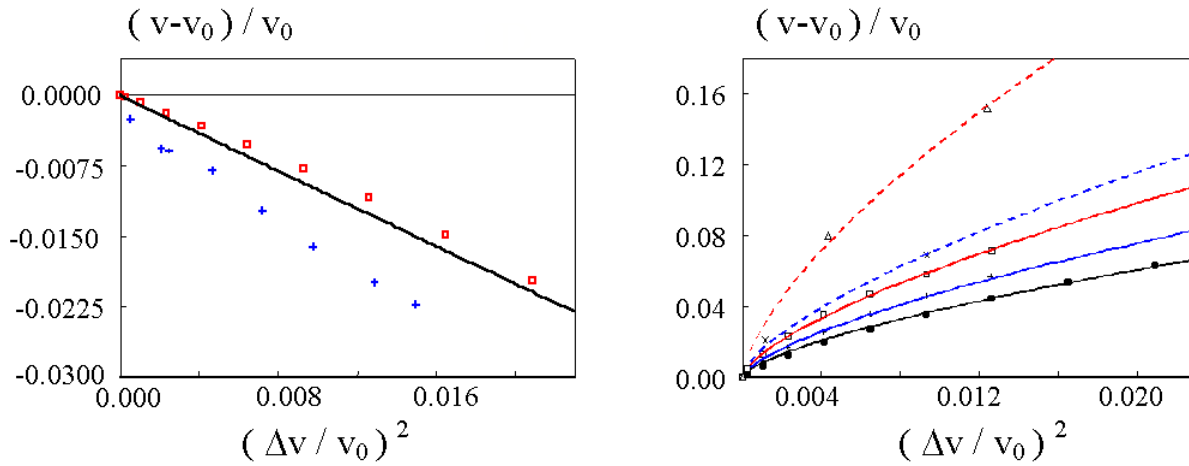


Fig. 4. Dependence of the relative variation in wave velocity versus amplitude disorder both numerically ($\phi_0 = 0.01$) and experimentally ($T_0 = 3.55 \text{ W/m}^2$). (a) One-dimensional system. Continuous line (slope -1) represents the theoretical prediction of Eq. (8). Numerical points (\square) were simulated with stripes of width 10 space units and the best linear fit corresponds to a slope of -0.93 ; experimental data ($+$) were obtained with squares of length of 1.1 cm and adjusted to a line of slope -1.42 . (b) Two-dimensional system. Numerically: for a medium width of 160 space units and noise squares of side length 10 (\bullet), 20 ($+$) and 40 (\square). Continuous lines represent nonlinear fits of Eq. (11), with $\beta = 0.831, 1.04$ and 1.35 , respectively. The typical front width is about 2.5 s.u. Experimental results are shown for a medium width of 5.4 cm and $l = 2.3 \text{ mm}$ (\times), and for 6 cm and $l = 2.7 \text{ mm}$ (\triangle), with $\beta = 1.59$ and 2.89 , respectively. Model parameters: $f = 3$, $q = 0.002$, $\varepsilon = 0.05$, $D_u = 1$, $D_g = 0$, $\phi_0 = 0.01$.

$T(x, y)$ in Sec. II varies slightly with the disorder amplitude. In Fig. 4(b) the 2D situation is plotted. The observed power laws and corresponding exponent are certainly consistent with the theoretical prediction, whereas the prefactor β in Eq. (11) is clearly seen to depend on the length scale of the spatial inhomogeneities. In any case, the distinctive behaviors depending on the dimension considered are clearly exhibited in the experiments.

4. Random Dichotomic Distribution of the Excitability with Nonexcitable Clusters

When one of the two values of the previous dichotomic distribution is set in the nonexcitable region, percolation phenomena can arise if the number of excitable sites is allowed to vary. In Fig. 3, the time evolution of a single experiment for a given proportion of dark squares (excitable) p is shown. Arrows indicate time evolution. In the first panel, the planar front is initiated at the bottom of the medium. The front breaks up into several parts that propagate along the lattice (second panel). And finally, only one of them reaches the upper side first (third panel), whereas the others wander around the lattice until their total annihilation (last panel).

4.1. Percolation phenomena

The motion of the wave front described above has the same features as in the typical models in percolation of forest fires or disordered semiconductors [Stauffer & Aharony, 1994; Sahimi, 1994; Last & Thouless, 1971]. Namely, no successful wave propagation is found below a critical value p_c which depends on the connectivity of the lattice: $p_c = 0.4072$ when a wave front can propagate from a excitable site to the next neighbor (through the sides in common) and to the next-nearest neighbor (through the vertex in common), and $p_c = 0.5928$ when only propagation through excitable squares with a common side is possible. In both cases, for p below p_c there is no path of excitable squares connecting the bottom and top edges of the pattern. For p above p_c most of the black sites belong to the *infinite cluster*, and the wave velocity is approximately constant. And, just at the percolation threshold, p_c , a fractal path of neighboring black squares appears which connects bottom and top of the medium for the first time, either through the corners or common sides, $p_c \approx 0.4$, or only through the common sides, $p_c \approx 0.6$. The transit time (the time the wave takes to reach the upper side of the medium first) is larger than the one measured for values of p above p_c (as the percolating cluster is very different from a straight line).

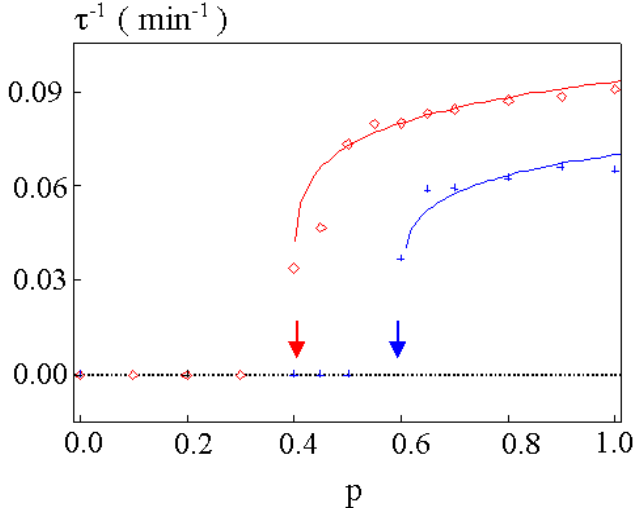


Fig. 5. Inverse of the transit time between both edges of the experimental system as a function of the probability of dark sites p . Continuous lines are nonlinear fits to Eq. (12) for p above the percolation threshold for two different geometries: (\square) cells connected by common sides, (\triangle) cells connected by common sides and corners. Parameters of the fitting curves are: (\triangle) $\alpha = 0.1$, $p_c = 0.4$. (\square) $\alpha = 0.08$, $p_c = 0.6$.

4.2. Results

Transit and termination times were measured for different values of the proportion p of squares with a given transmittance. Owing to the fact that the medium is finite, and in order to compare the results with theoretical predictions, five experiments were carried out for each value of p . The inverse of the transit time was plotted in Fig. 5 for the two spatial geometries. The experimental results for $p > p_c$ were fitted to a power law, typical of critical phenomena, with the critical exponent of $\beta = 5/36$ for a two-dimensional lattice [Stauffer & Aharony, 1994],

$$\tau^{-1} = \alpha(p - p_c)^\beta. \quad (12)$$

Zero values of the inverse of such an elapsed time naturally correspond to unsuccessful propagation.

The extinction time (the elapsed time until there is no wave activity in the medium) was calculated both experimentally (Fig. 6 top) and numerically (Fig. 6 bottom) as a function of p . Lifetimes of autowaves show a peak near $p \approx 0.5$ for the first geometry and at $p \approx 0.6$ for the second one. Note that, for $p \approx 0.6$, extinction times are larger than at $p \approx 0.5$ because light transmittance is higher, thus decreasing the wave velocity. The peaks are associated to the fractal properties of the connecting cluster at $p = p_c$ whose length is no longer linearly proportional to the length of the

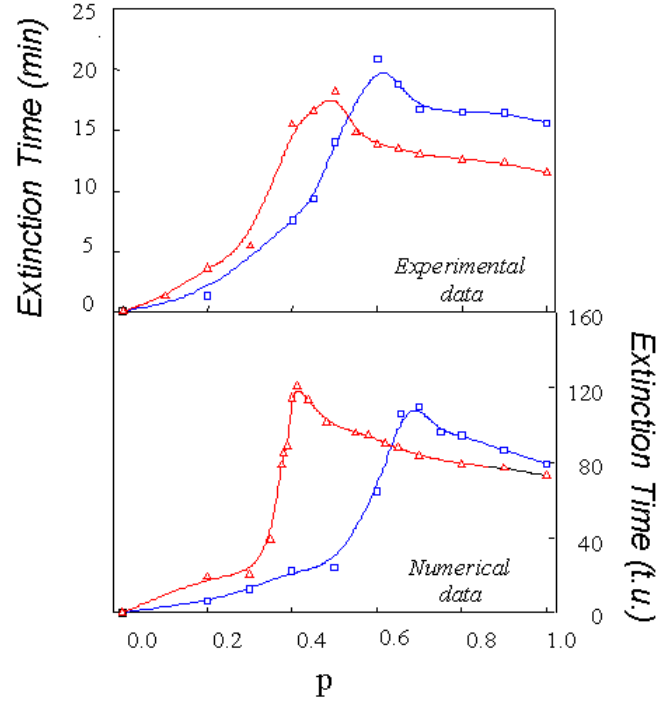


Fig. 6. Extinction time as a function of p , top: experimentally, bottom: numerically, for the two different lattice geometries (symbols have the same meaning as in Fig. 5). Solid lines are spline interpolations of the experimental and numerical data. (a) Experiments: Maxima located at (\triangle) $p_c \approx 0.5$, (\square) $p_c = 0.6$. Parameters as in Fig. 1. (b) Simulations: Maxima located at (\triangle) $p_c \approx 0.45$, (\square) $p_c = 0.6$. Model parameters: $f = 3$, $q = 0.002$, $\varepsilon = 0.05$, $D_u = 1$, $D_v = 0$, $\phi_b = 0.01(0.015)$, $\phi_w = 0.04(0.04)$ to reproduce $p_c \approx 0.45$, ($p_c = 0.6$).

lattice. Due to finite-size effects the peaks appear as being of finite height and with rounded shape. In fact, the value of $p \approx 0.5$ does not match exactly the threshold $p_c = 0.4072$ predicted by the theory. This is improved in numerical simulations where lattice sizes were larger. The critical values approach better to the expected values and the peaks are more pronounced.

5. Conclusions

Wave propagation through a two-dimensional medium with a static disordered excitability is observed to be distorted. Wave velocity is greater than the one corresponding to wave propagation through a medium with the equivalent mean excitability. From the eikonal equation modified with the fluctuating field of velocity a power-law dependence for the relative change of the propagation speed on the disorder amplitude is derived, which is verified both

experimentally and numerically. The opposite behavior is found when the wave fronts propagate in one dimension due to the lack of curvature effects. For this case, results are interpreted using simple kinematic arguments. With respect to the other considered situation, namely, wave propagation on a lattice of excitable and nonexcitable clusters, the effective wave front velocity is observed to jump from zero to finite values at a threshold $p = p_c$ (very close to the percolation thresholds expected for a square lattice). This occurs when, as predicted by the classical percolation theory, a cluster of sites with the same excitability spans the medium. These thresholds depend on the number of effective neighbors.

Acknowledgments

This work was partially supported by the Comisión Interministerial de Ciencia y Tecnología and Consellería de Educación e Ordenación Universitaria (Xunta de Galicia) under Project No. DGES-PB96-0937, PB96-1001 and PB96-0241, PB97-0540 and XUGA 20602B97.

References

- Agladze, K., Keener, J. P., Müller, S. C. & Panfilov, A. [1994] "Rotating spiral waves created by geometry," *Science* **264**, 1746–1748.
- Allesie, M. A., Bonke, F. M. I. & Scopman, T. Y. G. [1973] "Circus movement in rabbit atrial muscle as a mechanism in tachycardia," *Circ. Res.* **33**, 54–62.
- Amaral, L. A. N., Barabasi, A.-L. & Stanley, H. E. [1994] "Universality classes for interface growth with quenched disorder," *Phys. Rev. Lett.* **73**, 62–65.
- Armero, J., Lacasta, A. M., Ramírez-Piscina, L., Casademunt, J., Sancho, J. M. & Sagués, F. [1996] "Pattern and velocity selection of fronts propagating in modulated media," *Europhys. Lett.* **33**, 429–434.
- Armero, J., Lacasta, A. M., Ramírez-Piscina, L., Casademunt, J., Sancho, J. M. & Sagués, F. [1996] "Front propagation in spatially modulated media," *Phys. Rev.* **E56**, 5405–5412.
- Barabasi, A. L. & Stanley, H. E. [1995] *Fractal Concepts in Surface Growth* (Cambridge University Press, Cambridge).
- Edwards, S. F. & Wilkinson, D. R. [1982] "The surface statistics of a granular aggregate," *Proc. R. Soc. London* **A381**, p. 17.
- Family, F. & Vicsek, T. [1991] *Dynamics of Fractal Surfaces* (World Scientific, Singapore).
- Gammaitoni, L., Hänggi, P., Jung, P. & Marchesoni, F. [1998] "Stochastic resonance," *Rev. Mod. Phys.* **70**, 223–287.
- Gómez-Gesteira, M., del Castillo, J. L., Vázquez-Iglesias, M. E., Pérez-Muñuzuri, V. & Pérez-Villar, V. [1994] "Influence of the critical curvature on spiral initiation in an excitable medium," *Phys. Rev.* **E50**, 4646–4649.
- Horsthemke, W. & Lefever, R. [1984] *Noise-induced Transitions* (Springer-Verlag).
- Jung, P. [1993] "Periodically driven stochastic systems," *Phys. Rep.* **234**, 175–295.
- Jung, P. & Mayer-Kress, G. [1995] "Spatiotemporal stochastic resonance in excitable media," *Phys. Rev. Lett.* **74**, 2130–2133.
- Kádár, S., Wang, J. & Showalter, K. [1998] "Noise-supported travelling waves in sub-excitable media," *Nature* **391**, 770–772.
- Kardar, M., Parisi, G. & Zhang, Y. C. [1986] "Dynamic scaling of growing interfaces," *Phys. Rev. Lett.* **56**, 889–892.
- Karma, A. [1993] "Spiral breakup in model equations of action potential propagation in cardiac tissue," *Phys. Rev. Lett.* **71**, 1103–1106.
- Kerstein, A. R. & Ashurst, Wm. T. [1992] "Propagation rate of growing interfaces in stirred fluids," *Phys. Rev. Lett.* **68**, 934–937.
- Krug, H. J., Pohlmann, L. & Kuhnert, L. [1990] "Analysis of the modified complete Oregonator accounting for oxygen sensitivity and photosensitivity of Belousov–Zhabotinsky systems," *J. Phys. Chem.* **94**, p. 4862.
- Last, B. J. & Thouless, D. J. [1971] "Percolation theory and electrical conductivity," *Phys. Rev. Lett.* **27**, 1719–1721.
- Maselko, J. & Showalter, K. [1991] "Chemical waves in inhomogeneous excitable media," *Physica* **D49**, 21–32.
- Meron, E. [1992] "Pattern formation in excitable media," *Phys. Rep.* **218**, 1–66.
- Muñuzuri, A. P., Davydov, V. A., Gómez-Gesteira, M., Pérez-Muñuzuri, V. & Pérez-Villar, V. [1996] "Frequency-modulated autowaves in excitable media," *Phys. Rev.* **E54**, R5921–R5924.
- Muñuzuri, A. P. & Markus, M. [1997] "Simple optical feedback loop: Excitation waves and their mirror image," *Phys. Rev.* **E55**, 33–35.
- Muñuzuri, A. P., Pérez-Muñuzuri, V. & Pérez-Villar, V. [1998] "Attraction and repulsion of spiral waves by localized inhomogeneities in excitable media," *Phys. Rev.* **E58**, R2689–R2692.
- Natterman, T., Stepanow, S., Tang, L.-H. & Leschhorn, H. [1992] "Dynamics of interface depinning in a disordered medium," *J. Phys. (Paris) II* **2**, 1483–1488.
- Pertsov, A. M., Wellner, M. & Jalife, J. [1997] "Eikonal relation in highly dispersive excitable media," *Phys. Rev. Lett.* **78**, 2656–2659.
- Ram-Reddy, M. K., Nagy-Ungvarai, Zs. & Müller, S.

- C. [1994] “Effect of visible light on wave propagation in the ruthenium-catalyzed Belousov–Zhabotinsky reaction,” *J. Phys. Chem.* **94**, 148–156.
- Sahimi, M. [1994] *Applications of Percolation Theory* (Taylor & Francis, London).
- Sendiña-Nadal, I., Gómez-Gesteira, M., Pérez-Muñuzuri, V., Pérez-Villar, V., Armero, J., Ramírez-Piscina, L., Casademunt, J., Sagués, F. & Sancho, J. M. [1997] “Wave competition in excitable modulated media,” *Phys. Rev.* **E56**, 6298–6301.
- Sendiña-Nadal, I., Pérez-Muñuzuri, A., Vives, D., Pérez-Muñuzuri, V., Casademunt, J., Ramírez-Piscina, L., Sancho, J. M. & Sagués, F. [1998a] “Wave propagation in a medium with disordered excitability,” *Phys. Rev. Lett.* **80**, 5437–5440.
- Sendiña-Nadal, I., Roncaglia, D., Vives, D., Pérez-Muñuzuri, V., Gómez-Gesteira, M., Pérez-Villar, V., Echave, J., Casademunt, J., Ramírez-Piscina, L. & Sagués, F. [1998b] “Percolation thresholds in chemical disordered media,” *Phys. Rev.* **E58**, R2689–R2692.
- Spach, M. S., Miller, W. T., Geselowitz, D. B., Borr, R. C., Kootsey, J. M. & Johnson, E. A. [1981] “The discontinuous nature of propagation in normal canine cardiac muscle: Evidence for recurrent discontinuities of intracellular resistance that affects membrane currents,” *Circ. Res.* **48**, 39–54.
- Starobin, J. M. & Starmer, C. F. [1996] “Boundary-layer analysis of waves propagating in an excitable medium: Medium conditions for wave-front-obstacle separation,” *Phys. Rev.* **E54**, 430–437.
- Stauffer, D. & Aharony, A. [1994] *Introduction to Percolation Theory* (Taylor & Francis, London).
- Tyson, J. J. & Keener, J. P. [1988] “Singular perturbation theory of travelling waves in excitable media (a review),” *Physica* **D32**, 327–361.
- Wang, J., Kádár, S., Jung, P. & Showalter, K. [1999] “Noise driven avalanche behavior in subexcitable media,” *Phys. Rev. Lett.* **82**, 855–858.
- Wellner, M. & Pertsov, A. M. [1997] “Generalized eikonal equation in excitable media,” *Phys. Rev.* **E55**, 7656–7661.
- Wiesenfeld, K. & Moss, F. [1995] “Stochastic resonance and the benefits of noise: From ice ages to crayfish and squids,” *Nature* **373**, 33–36.
- Yamaguchi, T., Kuhnert, L., Nagy-Ungvaray, Zs., Müller, S. C. & Hess, B. [1991] “Gel systems for Belousov–Zhabotinsky reaction,” *J. Phys. Chem.* **95**, 5831–5837.
- Zhang, J., Zhang, Y.-C., Alstrøm, P. & Levinsen, M. T. [1992] “Modeling forest fire by a paper-burning experiment, a realization of the interface growth mechanism,” *Phys.* **A189**, 383–389.
- Zykov, V. S. [1980] “Analytical evolution of the dependence of the speed of an excitation wave in a two-dimensional excitable medium on the curvature of its front,” *Biophysics* **25**, 811–906.

